Latest developments on the shielding effectiveness measurements of materials and gaskets in reverberation chambers

POST PRINT VERSION

Title: Latest developments on the shielding effectiveness measurements of materials and gaskets in reverberation chambers
Authors: Angelo Gifuni, Gabriele Gradoni, Christopher Smartt, Steve Greedy, Armando M. Villalón, Luca Bastianelli, Franco Moglie, Valter Mariani Primiani, Stefano Perna, David Thomas
Journal: IET Science, Measurement & Technology
Publisher: John Wiley and Sons

DOI: 10.1049/iet-smt.2019.0242
Editor Website: https://ietresearch.onlinelibrary.wiley.com/doi/10.1049/iet-smt.2019.0242

ISSN 1751-8822
Received Date: 17th May 2019
Accepted Date: 9th December 2019
Available online: 1 June 2020

Please cite this article as:
Gifuni, A., Gradoni, G., Smartt, C., Greedy, S., Villalón, A.M., Bastianelli, L., Moglie, F., Mariani Primiani, V., Perna, S. and Thomas, D. (2020), Latest developments on the shielding effectiveness measurements of materials and gaskets in reverberation chambers. IET Sci. Meas. Technol., 14: 435-445. https://doi.org/10.1049/iet-smt.2019.0242

IET Science, Measurement & Technology

Research Article

IET Journals
The Institution of Engineering and Technology

Latest developments on the shielding effectiveness measurements of materials and gaskets in reverberation chambers

ISSN 1751-8822
Received on 17th May 2019
Revised 25th October 2019
Accepted on 9th December 2019
doi: 10.1049/iet-smt.2019.0242
www.ietdl.org

Angelo Gifuni[1] ✉, *Gabriele Gradoni*[2,3], *Christopher Smartt*[2], *Steve Greedy*[2], *Armando M. Villalón*[2], *Luca Bastianelli*[4], *Franco Moglie*[4], *Valter Mariani Primiani*[4], *Stefano Perna*[1], *David Thomas*[2]

[1]*Dipartimento di Ingegneria, Università di Napoli Parthenope, Centro Direzionale di Napoli, Napoli, Italy*
[2]*George Green Institute for Electromagnetics Research, University of Nottingham, NG7 2RD, UK*
[3]*School of Mathematical Sciences, University of Nottingham, NG7 2RD, Nottingham, UK*
[4]*Dipartimento di Ingegneria dell'Informazione, Università Politecnica delle Marche, Via Brecce Bianche 12, Ancona, Italy*
✉ *E-mail: angelo.gifuni@gmail.com*

Abstract: In this study, the authors present the latest developments on the measurements for the shielding effectiveness (SE) of gaskets and materials in reverberation chambers (RCs). A variant method, where the insertion loss of the fixture is achieved from the SE of the fixture with no sample in the aperture is found; it is appropriate for gaskets and for any flat material having a sufficiently high reflectivity at least on one side. A simple and usable condition under which the simplest method for the SE measurements of gaskets and materials in RCs can be used is also given, as well as particular cases where it can be directly applied are shown. This method, whose applicability is enhanced in this study, can be used for gaskets and any flat sample. Such developments simplify measurement setup and associated procedures. Comparisons of results support the methods for the SE measurements of gaskets and material in RCs shown in this study.

1 Introduction

Reverberation chambers (RCs) are used for shielding effectiveness (SE) measurements [1–9]. In particular, SE of gaskets and materials are made by using nested RCs (NRCs) [1, 2, 4, 8, 9]; contiguous reverberation chambers (CRCs) can also be used [8, 9]. It is meant that materials and gaskets include any flat electronic system such as printed circuit board (PCB), PCB assembly (PCBA) etc. According to a recent study, the standard procedure for the SE measurements of gaskets and materials in RCs, which is shown in IEC 64000-4-21 [1], can be improved [10]. In this paper, some developments of the improved measurement method shown in [10], are shown in order to simplify the measurement setup and associated procedures. A variant of the improved method [10] using a single antenna in the fixture is found. For such a variant procedure, insertion loss (IL) of the fixture is achieved from the SE of the fixture with no sample in the aperture; therefore, the mechanical stirring in the fixture is not strictly required. The single antenna in the fixture works only as a receiving antenna. This variant procedure is appropriate for gaskets and for any flat material having a sufficiently high reflectivity at least on the side where the field impinges from the fixture. Below, the expression 'sufficiently high reflectivity' will be quantitatively made clear. This case generally includes complex PCBs and complex PCBAs. The SE for this variant procedure is denoted by SE_5 in this paper. We also show and discuss a simple and usable condition under which the simplest model for SE measurements of gaskets and materials can be used. This procedure was formally introduced in [4, (14)], where it is denoted by SE_4; it is denoted in the same way in this paper. When the condition for its validity is met, it can be applied for any type of flat sample. It uses only two antennas and two transmission measurements; it is rapid and accurate. The only drawback is a possible moderate reduction of the measurement dynamic range (MDR). However, the applicability of SE_4 is strongly enhanced by this paper.

It is specified that a single antenna is also used in the fixture in [10]; but, the method of measurement is different as it uses reflection measurements and an enhanced backscatter constant e_b [11–13], and it assumes that $e_b = 2$ in the fixture itself. However, reflection measurements are critical with respect to transmission measurements, especially when the calibration plane has to be taken at end of a long cable and when values to be measured are very low, as it is frequently the case for SE measurements by NRCs. In fact, movements of cables and stress to cable and connector considerably affect reflection measurements. The validity of the method SE_5 and of the simple and usable condition for the applicability of SE_4, as well as the validity of an intermediate method, which is seen below, is shown by measurements. Note that the symbols SE_4, SE_5, as well as other similar symbols are used to denote the concerning measurement methods.

The paper is organised as follows: in Section 2, background is shown; in Section 3, the theory and an in-depth analysis are shown; in Section 4, results are shown; finally, in Section 5, the conclusions are drawn.

2 Background

In [4], a systematic method for SE measurements of gasket and materials was introduced, which is valid under a specified condition of isolation between the chambers [9]. It is denoted by SE_3. It clarifies the differences in the results from the two previous and incomplete methods [2, 3], which are denoted by SE_1 and SE_2. Note that the methods SE_1, SE_2, and SE_3 are denoted in the same way both in [4] and in [10], as well as in this paper [In this connection, we specify that in the formula expressing SE_1 after (7b) in [10], an equals sign have to be put after the symbol $SE_{fixt,s}$; its lack was clearly due to a clerical error.]. A sketch of NRCs and CRCs, where all four antennas are present, is shown in Figs. 1 and 2, respectively, in order to improve the readability of the necessary detailed background.

In the standard IEC 64000-4-21, the procedure and concerning formula [1, eq. (G.5)] is not supported by the theory [4, 10]. The improvement of the procedure for SE includes two cases [10, Sections 2 and 4]: case *A*, where the condition on the isolation between the chambers, that is formally expressed in [10, (6)], has to be met with the sample in the aperture and where the aperture size could also be of the order of a full side of the fixture; case *B*,

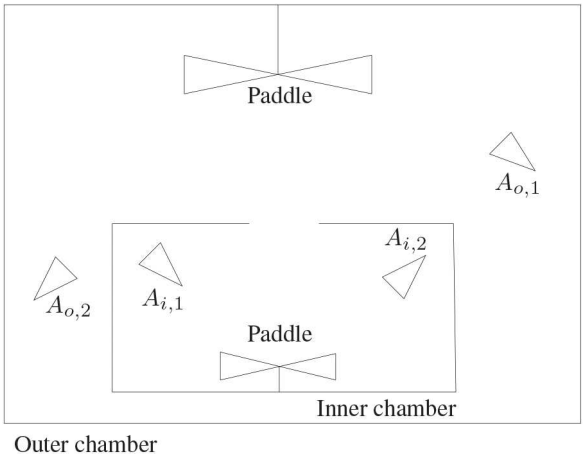

Fig. 1 *NRC when all four antennas are present: two outer antennas* $(A_{o,1}, A_{o,2})$ *and two inner antennas* $(A_{i,1}, A_{i,2})$

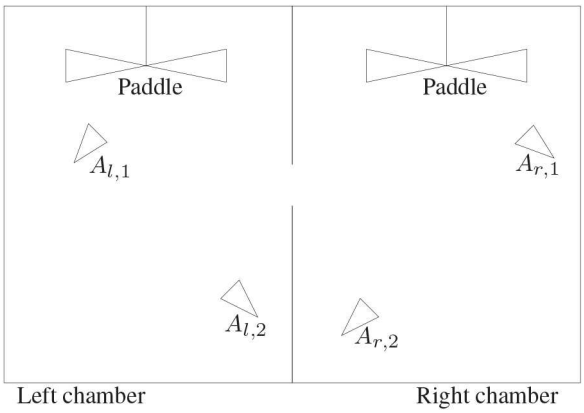

Fig. 2 *Contiguous RC when all four antennas are present: two left antennas* $(A_{l,1}, A_{l,2})$ *and two right antennas* $(A_{r,1}, A_{r,2})$

where the condition on the isolation has to be met with no sample in the aperture. In the latter case, the aperture size is limited by the condition of isolation itself even though the aperture has to however be electrically large.

Considering the above, it is recalled that the method in [10, (1)] can be applied for both cases *A* and *B* according to the isolation conditions to be met [Note that in [10, (1)], TFVF1 was wrongly written as 'TFVN1'. It was clearly a clerical error.]. Note that the condition on the isolation for the case *A* in [10] is the same as that in [4] (with the sample in the aperture), and that for the case *B* in [10], it is the same as that in [4] (with no sample in the aperture). In any case, the average transmission cross section (TCS) of the aperture is well-approximated by the geometrical optics as it is electrically large. It is equal to $A_a/4$, where A_a is the geometrical area of the aperture. The isolation between the chambers is required to be greater than or equal to 10 dB both with the sample in the aperture and with no sample in the aperture, [1, 9]. Such a condition, which is shown in detail in [9], is certainly met when the sufficient condition is met. The sufficient condition is formally expressed in [10, (5)] for the sample in the aperture. The corresponding condition for no sample in the aperture is overall similar. The latter depends on the aperture dimensions and on the volume of the fixture, as well as on its load. When the isolation with no sample in the aperture is not met and the method to be used requires it, the error in the SE measurements, which depends both on the isolation with no sample and on the isolation with sample, can be read in [9, Fig. 2].

For better readability of this paper, the conditions on the isolation between the chambers are shown below, as well as the corresponding sufficient conditions. They are written also in terms of ILs. We can write [9] [Note that some authors use a definition of IL such that its value in dB is negative [10], as is the case here.]:

$$\mathrm{I_{ns}} = -10\log\left(\frac{P^{\mathrm{o}}_{rx,\mathrm{i,ns}}}{P^{\mathrm{o}}_{rx,\mathrm{o,ns}}}\frac{P^{\mathrm{i}}_{rx,\mathrm{o,ns}}}{P^{\mathrm{i}}_{rx,\mathrm{i,ns}}}\right) = 10\log\left(\frac{\mathrm{IL_{o,o,ns}}}{\mathrm{IL_{o,i,ns}}}\frac{\mathrm{IL_{i,i,ns}}}{\mathrm{IL_{i,o,ns}}}\right) \quad (1)$$

$$= 10\log(\mathrm{SE_{fixt,ns}}) + 10\log\left(\frac{\mathrm{IL_{fixt,ns}}}{\mathrm{IL_{i,o,ns}}}\right) \geq 10\ \mathrm{dB},$$

$$\mathrm{SE_{fixt,ns}} = 10\log(\mathrm{SE_{fixt,ns}}) \geq 5\ \mathrm{dB} \quad \text{(sufficient condition for (1))}, \quad (2)$$

$$I_{\mathrm{s}} = -10\log\left(\frac{P^{\mathrm{o}}_{rx,\mathrm{i,s}}}{P^{\mathrm{o}}_{rx,\mathrm{o,s}}}\frac{P^{\mathrm{i}}_{rx,\mathrm{o,s}}}{P^{\mathrm{i}}_{rx,\mathrm{i,s}}}\right) = 10\log\left(\frac{\mathrm{IL_{o,o,s}}}{\mathrm{IL_{o,i,s}}}\frac{\mathrm{IL_{i,i,s}}}{\mathrm{IL_{i,o,s}}}\right) \quad (3)$$

$$= 10\log(\mathrm{SE_{fixt,s}}) + 10\log\left(\frac{\mathrm{IL_{fixt,s}}}{\mathrm{IL_{i,o,s}}}\right) \geq 10\ \mathrm{dB},$$

$$\mathrm{SE_{fixt,s}} = 10\log(\mathrm{SE_{fixt,s}}) \geq 5\ \mathrm{dB} \quad \text{(sufficient condition for (3))}. \quad (4)$$

The subscripts s and ns mean 'with sample' and 'with no sample' in the aperture, respectively; therefore, the interpretation of the corresponding parameters is consequential.

It is specified that $P^{\mathrm{o}}_{rx,\mathrm{o,ns}}$ is the average power received by an antenna in the outer chamber when the nested system is fed by the outer chamber; $P^{\mathrm{o}}_{rx,\mathrm{i,ns}}$ is the average power received by an antenna in the inner chamber when the nested system is fed by the outer chamber; $P^{\mathrm{i}}_{rx,\mathrm{i,ns}}$ is the average power received by an antenna in the inner chamber when the nested system is fed by the inner chamber; $P^{\mathrm{i}}_{rx,\mathrm{o,ns}}$ is the average power received by an antenna in the outer chamber when the nested system is fed by the inner chamber; $\mathrm{IL_{o,o,ns}}$ is the IL of the outer chamber with no sample in the aperture; $\mathrm{IL_{o,i,ns}}$ is the IL measured between the outer and inner chambers with no sample in the aperture; $\mathrm{IL_{fixt,ns}} = \mathrm{IL_{i,i,ns}}$ is the IL of the fixture; $\mathrm{SE_{fixt,ns}} = \mathrm{IL_{o,o,ns}}/\mathrm{IL_{o,i,ns}}$ is the SE of the fixture with no sample in the aperture. The notation for all parameters with sample in the aperture is obvious; for example, we have $\mathrm{SE_{fixt,s}} = \mathrm{IL_{o,o,s}}/\mathrm{IL_{o,i,s}}$, where $\mathrm{IL_{o,o,s}}$ is the IL of the outer chamber with sample in the aperture and $\mathrm{IL_{o,i,s}}$ is the IL measured between the outer and inner chambers with the sample in the aperture. It is important to note that the ratios of received powers can be read as ratios of ILs, as the corresponding transmitting powers can on average be considered constant. For sake of simplicity, hereinafter, the ratios of power are written in terms of ILs only. Note also that $\mathrm{IL_{o,i,ns}} = \mathrm{IL_{i,o,ns}}$ and $\mathrm{IL_{o,i,s}} = \mathrm{IL_{i,o,s}}$ from reciprocity.

2.1 Background for SE_5 using a single aperture

Two essential conditions have to be met to apply the method SE_5: (*a*) a fixture having an electrically large aperture (ELA) that meets the condition (1); (*b*) a sample for which it turns out that $\mathrm{IL_{fixt,s}} \cong IL_{\mathrm{fixt,pec}}$, where $\mathrm{IL_{fixt,pec}}$ is the IL of the fixture when the aperture is totally covered by a metallic plate. The condition $\mathrm{IL_{fixt,s}} \cong \mathrm{IL_{fixt,pec}}$ clarifies the meant of 'sufficiently high reflectivity' for a sample. Such a condition is considered met from the choice of the samples; this rationale is supported by the fact that $\mathrm{IL_{fixt,s}}$ is not very sensitive for small absorptions of the sample in the aperture and/or for the leakage from its edge. For symmetrical samples from the point of view of the reflectivity, the implication $\mathrm{IL_{o,o,s}} \cong \mathrm{IL_{o,o,pec}} \Rightarrow \mathrm{IL_{fixt,s}} \cong \mathrm{IL_{fixt,pec}}$ could be used even though it becomes practically weak for apertures physically very small and very large outer chamber. Finally, a preliminary absorption measurement [1, 14–20] or a preliminary reflectivity measurement could be made [21]. The condition (1) is necessary only to achieve $\mathrm{IL_{fixt,pec}}$ by the SE of the fixture (enclosure) with no sample in the aperture, which in turns allows the SE of the sample to be obtained by using a single antenna in the fixture when the condition (b) is also met, as further specified in the next

section. Measurements to verify the necessary condition (1) are included in those necessary to obtain the SE of the sample. It is specified that the ELA is arranged with a sample holder which depends on the sample type; it minimises the leakage from the edge of the sample and consequently the MDR increases.

2.2 Background for SE_5 using an 'Auxiliary ELA'

In the previous subsection, since the condition (1) is necessary only to achieve $IL_{fixt,pec}$ as mentioned above, in the procedure for SE_5, the size of the aperture with no sample can also be less than that of the aperture with sample. In fact, when the aperture with a sample holder, i.e. the aperture where the sample is mounted, does not meet the condition (1), then it can appropriately be reduced by covering it by an aluminium tape or an aluminium sheet. Such a reduced aperture is called the 'auxiliary ELA (AELA)' in this paper. Clearly, the AELA, which is always an aperture with no sample, has to meet the condition (1). In this case, the aperture with sample, which has different size than the aperture with no sample (AELA), has to meet the condition (3). The condition (*b*) $IL_{fixt,s} \cong IL_{fixt,pec}$ has to however be met. Measurements to verify the necessary conditions (1) and (3) are included in those necessary to obtain the SE of the sample also in this case. In particular, it is specified that when the sufficient condition (4) is not met, then $IL_{fixt,s}$ is replaced with $IL_{fixt,pec}$ in (3), which can be obtained by $SE_{fixt,ns}$, as shown below.

In the standard, it is expected that the smallest dimension of the fixture aperture should be at least $\lambda/2$ at the lowest usable frequency (LUF) in order to minimise the cutoff effect; λ is the wavelength of the electromagnetic radiation. Note that the blocking effect depends also on the thickness of the sample holder, which in turn depends on the specific sample: the greater the thickness (in terms of λ), the greater is the blocking effect. Normally, the thickness of a sample holder is much less of the maximum λ value. However, we note that no sample holder is necessary for an AELA. In Section 4, we will show by measurements that a square aperture, whose side is a little less than $\lambda/2$ long, could be used as a large aperture.

In [22] a square aperture of the side length of about $0.3\lambda_{max}$ is used. Analytical model for of transmission coefficients of aperture for a specific polarisation and incident direction are available in the literature [23, 24]. Finally, note that the frequency range (FR) is determined by the AELA. However, samples greater than the AELA can be used according to the size of the aperture with sample.

2.3 Brief considerations for both methods SE_5

The fixture is always randomly fed from the outer chamber for both versions of the method SE_5; therefore, the mechanical stirring in the fixture is not strictly necessary, i.e. only frequency stirring (FS) can be used. It is stressed that for both versions of the method SE_5, a single antenna is necessary in the fixture. If a load is added in the fixture, in order to achieve the requested isolation conditions, it has to remain throughout the whole measurement procedure. Moreover, it has to be carefully chosen in order to avoid unacceptable non-uniformity of the field inside the fixture itself. Clearly, the SE of any ELA with no sample (clearly, including any AELA) considered in this paper is assumed to be equal to 0 dB.

2.4 Background for the methods SE_4 and SE_6

Measurements of SE of gaskets and materials can be made by using only two antennas when the quality factors Q_o and Q_i of the two chambers (outer and inner chambers, respectively) remain practically constant with no sample and with sample in the aperture. In this case, the simplest method SE_4 can be used. From theory in [4, 9], we find a simple and usable condition for the applicability of SE_4. For such a derivation, an intermediate method is also found for SE measurements; this method is denoted by SE_6 in this paper. It is appropriate in cases where the IL_s of the outer chamber with sample and with no sample in the aperture are practically equal and the IL of the fixture with sample in the aperture is practically equal to that of the fixture with a metallic slab in the aperture. We will see that SE_6 is less useful than SE_5 and SE_4.

3 Theory

In this section, the theory for the method SE_5 and for the simple and usable condition for the applicability of SE_4 is shown. The theory for SE_6 is also included. Since the theory for SE_5 is the same both when the AELA is used and when it is not used, as shown above, no difference is highlighted in the nomenclature between the two cases. However, the cases where the AELA is necessary and those where it is not necessary are well specified according to the considerations in the previous section.

3.1 Theory for the method SE_5

In this section, we show that when the condition (3) and (b) are met, $IL_{fixt,pec}$ can be achieved by $SE_{fixt,ns}$. If the condition (3) is met, then we can write [10]:

$$\begin{aligned} SE_{ap} &= 10\log\left(\frac{A_a/4}{\sigma_{t,ns}}\right) \\ &= 10\log\left(\frac{IL_{o,o,ns}}{IL_{o,i,ns}}\right) + 10\log\left(\frac{A_a/4}{A_e}\right) + 10\log(IL_{fixt,ns}). \end{aligned} \tag{5}$$

Note that the first term in (5) is equal to $SE_{fixt,ns}$. The average TCS, i.e. $A_a/4$, is equal to a perfectly absorption cross-section (ACS) [14–20]; $A_e = \lambda^2 8\pi$ is the average effective area of an antenna in an RC [14, 15, 19]. Note also that in this paper, the parameters are shown both in dB and in absolute value; the context makes clear if a parameter is in dB or in absolute value. Under the abovementioned hypotheses, the SE of the aperture with no sample, which is denoted by SE_{ap}, can be assumed equal to one. By (5), we can write [25, 26]:

$$IL_{fixt,ns} = \frac{IL_{o,i,ns}}{IL_{o,o,ns}}\frac{A_e}{A_a/4} = \frac{1}{SE_{fixt,ns}}\frac{A_e}{A_a/4} \quad . \tag{6}$$

By using (6), the total ACS of the fixture can be calculated. We can write

$$ACS_{fixt,ns} = \frac{A_e}{IL_{fixt,ns}}, \tag{7}$$

where $ACS_{fixt,ns}$ is the total ACS of the fixture with no sample in the aperture [16, 23]. By using (6) and (7), we can achieve $IL_{fixt,pec}$. We can write:

$$IL_{fixt,pec} = \frac{A_e}{ACS_{fixt,ns} - A_a/4} = \frac{A_e}{A_a/4}\cdot\frac{1}{SE_{fixt,ns} - 1}. \tag{8}$$

It is specified that when (5)–(8) are referred to an AELA, the symbol A_a is meant as $A_{a,aux}$; the subscript 'aux' denotes the AELA. Note that (8) can be substituted with $IL_{fixt,s}$ in (3), as specified above. The reflecting samples, which can be tested by the method SE_5, include gaskets, complex PCBs, fabric shield [8], graphene shields [27], band-stop frequency selective surface [28, 29] etc. In such cases, (8) can be replaced in (5) when it is written for a sample in the aperture; that is, we can write [10]:

$$\begin{aligned} SE_5 &= 10\log\left(\frac{IL_{o,o,s}}{IL_{o,i,s}}\right) \\ &\quad + 10\log\left(\frac{A_a/4}{A_e}\right) + 10\log(IL_{fixt,pec}). \end{aligned} \tag{9}$$

It is highlighted that A_a in (9) is always referred to as the aperture with the sample. By using (6)–(8), (9) can be written as follows:

$$\mathrm{SE}_5 = 10\log(\mathrm{SE}_{\mathrm{fixt,s}}) + 10\log\left(\frac{A_\mathrm{a}}{A_{\mathrm{a,aux}}}\right) - 10\log(\mathrm{SE}_{\mathrm{fixt,ns}} - 1)\,. \tag{10}$$

where $\mathrm{SE}_{\mathrm{fixt,ns}}$, which [under condition (1)] is always greater than one, is referred to the AELA when it is used. Clearly, $\mathrm{SE}_{\mathrm{fixt,s}}$ is always referred to the aperture with sample. When an AELA is not necessary, then $A_\mathrm{a} = A_{\mathrm{a,aux}}$ and (10) simplifies. The ratio $A_\mathrm{a}/A_{\mathrm{a,aux}}$ is practically always greater than 1. Equation (10) is simple to implement as it does not require directly the application of (6)–(8), even though (9) has the same form of (1) in [10], which is similar to the form of the SE of gaskets and material in [1]. The form (10) highlights the fact that the procedure for SE_5 requires only three antennas. Considering the necessary conditions for the applicability of the method SE_5, we note that cases where the AELA is not necessary correspond to the case *B* in [10, Sections 2 and 4], whereas cases where the AELA is necessary correspond to the case *A* in [10, Sections 2 and 4] once $\mathrm{IL}_{\mathrm{fixt,pec}}$ is achieved.

3.2 Theory for a simple and usable condition for the applicability of the method SE_4

When the condition (1) is met, the model SE_3 for the SE of gaskets and materials is [4, 9]:

$$\begin{aligned}\mathrm{SE}_3 &= 10\log\left(\frac{\mathrm{SE}_{\mathrm{fixt,s}}}{\mathrm{SE}_{\mathrm{fixt,ns}}}\right) + 10\log\left(\frac{\mathrm{IL}_{\mathrm{fixt,s}}}{\mathrm{IL}_{\mathrm{fixt,ns}}}\right)\\ &= 10\log\left(\frac{\mathrm{IL}_{\mathrm{o,o,s}}}{\mathrm{IL}_{\mathrm{o,i,s}}}\right) + 10\log\left(\frac{\mathrm{IL}_{\mathrm{o,i,ns}}}{\mathrm{IL}_{\mathrm{o,o,ns}}}\right) + 10\log\left(\frac{\mathrm{IL}_{\mathrm{fixt,s}}}{\mathrm{IL}_{\mathrm{fixt,ns}}}\right).\end{aligned} \tag{11}$$

Note that the ratio of the net power supply can be considered equal to one. We achieve the required usable condition for the applicability of SE_4 by an intermediate step, which results in the method SE_6. If the conditions

$$\mathrm{IL}_{\mathrm{o,o,ns}} = \mathrm{IL}_{\mathrm{o,o,s}} \tag{12a}$$

$$\mathrm{IL}_{\mathrm{fixt,s}} = \mathrm{IL}_{\mathrm{fixt,pec}} \tag{12b}$$

are met, then we can write as follows:

$$\mathrm{SE}_6 = 10\log\left(\frac{\mathrm{IL}_{\mathrm{o,i,ns}}}{\mathrm{IL}_{\mathrm{o,i,s}}}\right) + 10\log\left(\frac{\mathrm{IL}_{\mathrm{fixt,pec}}}{\mathrm{IL}_{\mathrm{fixt,ns}}}\right)\quad. \tag{13}$$

The condition (12a) always holds when the total ACS of the outer chamber including the fixture with no sample in the aperture, which is denoted by $\mathrm{ACS}_{\mathrm{RC,ns}}$, is much greater than the ACS of the sample obtained when the field impinges from the outer chamber, whose maximum value is $A_\mathrm{a}/4$; namely, (12a) always holds when $\mathrm{ACS}_{\mathrm{RC,ns}} \gg A_\mathrm{a}/4$. It also holds when the ACS of the sample obtained when the field impinges by the outer chamber is about the same as that of the aperture with no sample.

The ILs $\mathrm{IL}_{\mathrm{o,o,ns}}$, $\mathrm{IL}_{\mathrm{o,i,ns}}$, and $\mathrm{IL}_{\mathrm{o,i,s}}$, which are required to apply (13), could be measured by using only two antennas; such $\mathrm{IL_s}$ determine the SE of the fixture [13]. However, such a procedure requires reflection coefficient measurements, which could become critical, as mentioned above. Similar considerations can be made for the method SE_5. We are interested in a simple usable condition under which $\mathrm{IL}_{\mathrm{fixt,ns}} \cong \mathrm{IL}_{\mathrm{fixt,pec}}$. Note that $\mathrm{IL}_{\mathrm{o,o,ns}} \cong \mathrm{IL}_{\mathrm{o,o,s}}$ does not necessarily imply $\mathrm{IL}_{\mathrm{fixt,ns}} \cong \mathrm{IL}_{\mathrm{fixt,s}}$ as mentioned above, whereas

$$\mathrm{IL}_{\mathrm{fixt,ns}} \cong \mathrm{IL}_{\mathrm{fixt,s}} \Rightarrow \mathrm{IL}_{\mathrm{o,o,ns}} \cong \mathrm{IL}_{\mathrm{o,o,s}}\quad. \tag{14}$$

In fact, if $\mathrm{ACS}_{\mathrm{fixt,ns}} \gg A_\mathrm{a}/4$, then $\mathrm{IL}_{\mathrm{fixt,ns}} \cong \mathrm{IL}_{\mathrm{fixt,pec}}$ and a fortiori $\mathrm{ACS}_{\mathrm{RC,ns}} \gg A_\mathrm{a}/4$; it follows that the condition on the left side of (14) is met. In this case, (11), as well as (13), results in

$$\mathrm{SE}_4 = 10\log\left(\frac{\mathrm{IL}_{\mathrm{o,i,ns}}}{\mathrm{IL}_{\mathrm{o,i,s}}}\right)\quad. \tag{15}$$

It is reaffirmed that SE_4 can be applied for any flat sample. By considering the condition on the left side of (14), one notes that (15), i.e. the method SE_4, can certainly be applied to samples having low reflectivity. For such a class of samples, the ACS of both sides is about the same as that of the aperture with no sample; such samples can also have a considerable SE value. Note that the condition of isolation expressed in (1), or that expressed in (2), is a necessary condition to apply SE_4 as it comes from SE_3.

The implication (14) is true also for two equal CRCs. By (6) and (7), we can write

$$\frac{\mathrm{ACS}_{\mathrm{fixt,ns}}}{A_\mathrm{a}/4} = \mathrm{SE}_{\mathrm{fixt,ns}}\,. \tag{16}$$

The $\mathrm{IL}_{\mathrm{fixt,s}}$ ranges from $\mathrm{IL}_{\mathrm{fixt,ns}}$ to $\mathrm{IL}_{\mathrm{fixt,pec}}$. We are interested in a simple and usable condition that approximates the ratio $\mathrm{IL}_{\mathrm{fixt,ns}}/\mathrm{IL}_{\mathrm{fixt,pec}}$ to 1, i.e. $\mathrm{IL}_{\mathrm{fixt,ns}} \cong \mathrm{IL}_{\mathrm{fixt,pec}}$. Note that the condition $\mathrm{IL}_{\mathrm{fixt,ns}} \cong \mathrm{IL}_{\mathrm{fixt,pec}}$, which is requested in the procedure for SE_4, is more stringent than the $\mathrm{IL}_{\mathrm{fixt,s}} \cong \mathrm{IL}_{\mathrm{fixt,pec}}$, which is requested in the procedure for SE_5. In fact, the former includes the latter. By using (16), (6), and (8), we can write

$$\frac{\mathrm{IL}_{\mathrm{fixt,ns}}}{\mathrm{IL}_{\mathrm{fixt,pec}}} = 1 - \frac{A_\mathrm{a}/4}{\mathrm{ACS}_{\mathrm{fixt,ns}}} = 1 - \frac{1}{\mathrm{SE}_{\mathrm{fixt,ns}}}\,. \tag{17}$$

If the ELA of the fixture, the volume, and the total losses are such that the SE of the enclosure ($\mathrm{SE}_{\mathrm{fixt,ns}}$) is greater than or equal to 4 (6 dB), then the conditions expressed by (14) are met and the ratio $\mathrm{IL}_{\mathrm{fixt,ns}}/\mathrm{IL}_{\mathrm{fixt,pec}}$ is less than or equal to 0.75 (–1.2 dB). Therefore, the model (15) can be applied under the condition as follows:

$$\mathrm{SE}_{\mathrm{fixt,ns}} \geq 4 = 6\,\mathrm{dB}\,. \tag{18}$$

We can write

$$\mathrm{SE}_{\mathrm{fixt,ns}} \geq 4 = 6\,\mathrm{dB} \Rightarrow \frac{\mathrm{IL}_{\mathrm{fixt,ns}}}{\mathrm{IL}_{\mathrm{fixt,pec}}} \geq 0.75 = -1.2\,\mathrm{dB}\,. \tag{19}$$

We note that under the condition (18), or equivalently (19), SE_4 can be applied with a maximum error of about 1 dB. It is noted that this error is a systematic error which is only a component of the measurement uncertainty (MU) [30], as it will be discussed in Section 3.4. Note that when the sufficient condition on the isolation is met with no sample in the aperture, (18) is roughly met. It is specified that the method SE_4 was used in [22] but there it was not adequately justified; however, we have found a simple and usable condition to check its applicability.

It is specified that the abovementioned considerations on a possible load added inside the fixture are valid also in this case. All measurements made with no sample can be considered calibration measurements for the fixture; therefore, they are made only once in a series of measurements where the configuration of the chambers changes only for the different sample types in the aperture.

3.3 Further in-depth analysis on the proposed methods and their measurement dynamic range

When (18) is met, we have an isolation with no sample of at least 12 dB; this occurs when the chambers are equal in volume, see (1) and (2). It is the minimum value of isolation (worst case) under the condition (18). Therefore, for the NRC, the isolation is normally >12 dB. Such an isolation causes just an error of some tenth of dB in the SE measurements [9, Fig. 2]. When (18) is met, (15) is equivalent to (11) and to [10, (1)]. Hence, when (18) is met and no AELA is used for SE_5, the methods SE_5 and SE_6 are also applicable apart from the sample absorption and reflectivity, and they give the same SE value as that given by SE_4 excepting for the

approximation in (17) due to the $SE_{fixt,ns}$ value in (19). As a consequence, the comparison of results from SE_5, SE_6, and SE_4 is an intrinsic validation for the three models. In Section 4.2, this criterion is used to validate the three methods. However, it is highlighted that in such cases it is convenient apply SE_4 for its greater simplicity. The method SE_6 is applicable to samples for which (12a) and (12b) are met. Both methods for SE_5 and SE_6 require three antennas, one of which is transmitting and two are receiving. One receiving antenna is placed inside the fixture; the transmitting antenna and the other receiving antenna are placed inside the outer chamber. The method SE_4 requires only two antennas and two IL measurements. The method SE_6 requires one fewer measurement with respect to SE_5, which is the measurement of $IL_{o,o,s}$. However, the method SE_5 has no reduction in MDR with respect to the corresponding methods improved in [10] and SE_6 has no reduction in MDR with respect to SE_3.

When the method SE_6 can be applied for a given sample and measurement setup, then the method SE_5 can certainly be applied to the same sample and measurement setup. It is specified that measurements for SE_6 and SE_4 are self-calibrating, whereas measurements for SE_5 (9) or equivalently (10) are not strictly self-calibrating, except for cases where the two receiving antennas are equal, as well as the total length of the cables connecting them to the instrumentation, as further specified in Section 4.2. In any case, SE_6 and SE_4 do not require corrections for antenna efficiency, as well as SE_5 when the two receiving antennas (in the outer and inner chambers) are equal.

It is important to note that for a given NRC system and under the condition $SE_{fixt,ns} \geq 6$ dB, the simplest model for SE_4 has a reduction of 6 dB in MDR with respect to the cases where the $SE_{fixt,ns}$ is about 0 dB. These can be the procedures where $IL_{fixt,ns}/IL_{i,o,ns}$ is about 10 dB, see (1), or those where the condition of isolation between the chambers has to be met with sample in the aperture. If the $SE_{fixt,ns} > 6$ dB, the MDR is reduced accordingly. We stress that the MDR can be increased by a reduction of the volume of the greater chamber.

One notes that SE measurements of an effective gasket represent reference measurements for SE of flat shields (materials). They represent the maximum SE measurable including the leakage of the fixture, which is meanly due to the sample holder, gasket, and closing system of the aperture (intensity and uniformity of the pressure for the electric contact) being the sample a metallic slab. SE measurements where the antenna inside the fixture is replaced with a well-shielded termination represent the maximum SE values that are potentially measurable, where no leakage from the fixture is present. Such maximum SE values represent the MDR when the minimum SE measurable is about 0 dB. Note that the measurements of the real potential MDR require a narrow intermediate frequency bandwidth (IFBW) of the vector network analyser (VNA).

The reference measurements from the gasket are obtained by applying the appropriate measurement methods; therefore, no other theoretical consideration is necessary. We show the MDR of SE measurements of the different methods where the receiving antenna inside the fixture is replaced with a well-shielded termination. The MDR of the improved method proposed in [10] and that of the method SE_5 have the same mathematical model; such an MDR is here denoted simply by MDR-SE. Measurements of $IL_{o,o,pec}$, $IL_{o,i,T}$, and $IL_{fixt,ns}$ are respectively considered, where the first two terms are the IL of the outer chamber when a metallic plate is in the aperture and the IL between the outer and inner chambers when a termination is connected to the reference plane of the antenna in the fixture. MDR-SE can be achieved as follows:

$$\begin{aligned} \mathrm{MDR-SE} = {} & 10\log\left(\frac{\mathrm{IL}_{o,o,pec}}{\mathrm{IL}_{o,i,T}}\right) \\ & + 10\log\left(\frac{A_a/4}{A_e}\right) + 10\log\left(\mathrm{IL}_{fix,pec}\right), \end{aligned} \tag{20}$$

where $IL_{o,o,pec}$ is the maximum value of $IL_{o,o}$; $IL_{o,i,T}$ is the minimum value of $IL_{o,i}$; $IL_{fixt,pec}$, is the maximum value of IL_{fixt}. Note that (20) is equivalent to the MDR achieved by considering (10), which is as follows:

$$\begin{aligned} \mathrm{MDR-SE} = {} & 10\log\left(\frac{\mathrm{IL}_{o,o,pec}}{\mathrm{IL}_{o,i,T}}\right) \\ & + 10\log\left(\frac{A_a}{A_{a,aux}}\right) - 10\log\left(\mathrm{IL}_{fix,ns} - 1\right). \end{aligned} \tag{21}$$

It is reaffirmed that $SE_{fixt,ns}$ is referred to the AELA when it is used. Similarly, for gasket measurements, the geometric area of the aperture is still considered to obtain the MDR [10, Section 2, subsection C]. For MDR-SE_4, we can write:

$$\mathrm{MDR-SE_4} = 10\log\left(\frac{\mathrm{IL}_{o,i,ns}}{\mathrm{IL}_{o,i,T}}\right). \tag{22}$$

It is important to note that MDR-SE_4 and MDR-SE are equal when the method SE_4 is applicable, as expected. In fact, when (18) is met, it can be shown that

$$\begin{aligned} \mathrm{IL}_{o,i,ns} &= \mathrm{IL}_{o,o,ns} \cdot ((A_a/4)/A_e) \cdot \mathrm{IL}_{fixt,ns} \\ &= \mathrm{IL}_{o,o,pec} \cdot ((A_a/4)/A_e) \cdot \mathrm{IL}_{fixt,pec} \end{aligned}$$

according to the $SE_{fixt,ns}$ value in (19).

3.4 On the MU of the proposed models

The MU includes both systematic and random errors [30]. The MU for SE can be calculated from each measurement model, by considering the MU of the single parameters in it included, as shown in [21, 31–34] for quantities different than SE. In [35, 36], the MU of the IL including FS and statistical non-uniformity is also shown. The effects of non-uniformity are also addressed in [37]. In proposed models for SE, are included both ILs of single chambers and ILs between two chambers. The MU for the IL was generalised in [36]. That is, it can be obtained without the knowledge of the statistical distribution of the acquired samples for the transmission coefficient of the chamber or between the two chambers [36]. Such an MU can be obtained both with FS and with no FS. Moreover, the distribution of ILs between two chambers can be easily achieved in our case as the RCs are coupled by a large aperture [38–41]; when the sample is present in the aperture, it can be considered equivalent to a case of many apertures as shown in [38]. In this paper, the uncertainty for proposed models of SE is not calculated for brevity.

4 Measurements and results

In this section, the results of SE from measurements acquired in different RCs and using different material samples are shown. Results from measurements made in RCs at Università Politecnica Delle Marche, Ancona, Italy, at the University of Nottingham, Nottingham, England, as well as results on a gasket from measurements at Università Parthenope, Napoli, Italy are shown. Results shown in this section include the verification of the LUF for an AELA. For this verification, measurements from RC in Ancona are used.

4.1 SE results from measurements made by using RC at Università Politecnica delle Marche, Ancona, Italy

The outer RC has dimensions of $6 \times 4 \times 2.5\,\mathrm{m}^3$ and the inner chamber has dimensions of $1.2 \times 0.9 \times 0.8\,\mathrm{m}^3$ [42, 43]. Inside the outer chamber, the input electromagnetic field is randomised by means of hybrid stirring using two metallic stirrers, which work in step mode for measurements used in this paper, and FS, whereas inside the inner chamber only FS is used. The measurement setup includes a four-port VNA, model Agilent 5071B, two antennas inside the outer chamber, model Schwarzbeck Mess-Elektronik

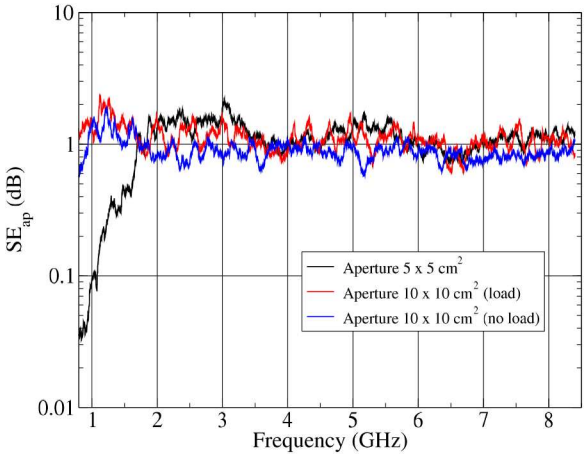

Fig. 3 *SE_{ap} of two apertures with no sample. For the aperture $10 \times 10\,cm^2$, the SE_{ap} is obtained both with load and no load in the fixture. The load is one pyramidal absorber (Eccosorb VHP-8-NRL by Emerson & Cuming). Cutoff effect is visible for frequencies less than about 2 GHz for the aperture $5 \times 5\,cm^2$. Such an effect is present for frequencies less than about 1 GHz for the aperture $10 \times 10\,cm^2$ even though it is not represented in a visible way in the figure*

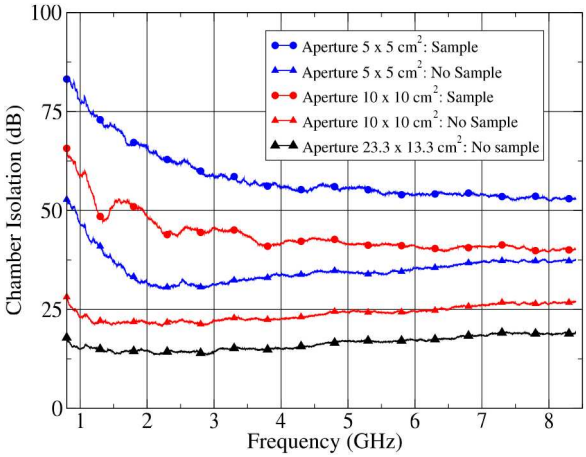

Fig. 4 *I_{ns} and I_s. Coefficients of isolation between the chambers for two apertures with no sample and with sample in the aperture. Only I_{ns} is shown for a third aperture of size $23.3\,cm \times 13.3\,cm$*

USLP 9143, whose usable FR ranges from 250 MHz to 8 GHz for EMC tests, and two antennas inside the inner chamber. The latter two antennas are a double-ridged horn antenna from AH Systems, model SAS-571, whose usable FR ranges from 700 MHz to 18 GHz for EMC tests, and a homemade discone antenna, which works well in the FR from 1 to 10 GHz. Measurements are acquired in the FR from 0.8 to 8.2 GHz; by automation, 16,000 samples are acquired for each position of the stirrers; the step frequency (SF) is 250 kHz. The IFBW and source power are set to 3 kHz (unless otherwise specified in the captions of the figures) and 0 dBm, respectively.

The total number of stirrer positions, which corresponds to the total number of (frequency) sweeps (M) is 64. In this section, SE results from methods SE_5 and SE_4 are compared to SE_3, in order to validate the procedures for the former methods. Since SE_3 is also applied, the measurement system is fully calibrated at the reference planes of the four antennas and samples of the necessary reflection and transmission coefficients are acquired both when the system is fed by the outer chamber and by the inner one [4, 5, 9]. In short, the two antennas in the two chambers can be both transmitting and receiving antennas. All measurements are appropriately corrected for total antenna efficiencies. To that end, it is specified that the radiation efficiencies used for such corrections are 0.7 for the two Log Periodic antennas and 0.9 for both the horn and the discone antenna. The radiation efficiencies are roughly considered constant in the measurement FR [1]. It is specified that results from method SE_6 are omitted in this section as results from SE_3 are shown and used to validate results from SE_5 and SE_4.

Results for the verification of the LUF of an AELA are shown first. For such purpose, we consider two apertures of size $5\,cm \times 5\,cm$ and $10\,cm \times 10\,cm$, respectively. These apertures are situated at the centre of an aluminium slab that covers a larger aperture provided with a sample holder, which is formed by a metallic frame [42, 43]. The thickness of the side where the aperture is present is less than 1 mm. Moreover, measurements using the aperture of $10\,cm \times 10\,cm$ are also accomplished with a load in the inner chamber, which is one pyramidal absorber (Eccosorb VHP-8-NRL by Emerson & Cuming), in order to achieve the necessary conditions to test the method SE_4 by such an aperture as well. Two examples of SE of apertures with no sample are shown in [4] and in [10]; in the latter case, the aperture has no sample holder. The SE_{ap} is obtained by (5); clearly, for the verification of the LUF of an AELA, which is not necessary to repeat for ordinary measurements of SE, $IL_{fixt,ns}$ has to be measured by using two antennas in the fixture. It is specified that the FS bandwidth (FSB) used for data processing is 400 frequency points, which corresponds to 100 MHz.

Fig. 3 shows the SE of the abovementioned AELAs for the verification of the corresponding LUFs. Results show that a square AELA of the side length of about $0.35\lambda_{max}$ can be used for SE measurements. In other words, the cutoff effect is present for frequencies less than about 2 GHz for the aperture $5 \times 5\,cm^2$ and for frequencies less than about 1 GHz for the aperture $10 \times 10\,cm^2$ even though the latter is not represented in a visible way in Fig. 3.

The apertures of $5\,cm \times 5\,cm$ and $10\,cm \times 10\,cm$ are used to test the method SE_5, both when an AELA is used and not used, and SE_4 under the obtained condition (18) or equivalently (19). To test the method SE_4 both the apertures of size $5\,cm \times 5\,cm$ and $10\,cm \times 10\,cm$ are arranged with an aluminium mesh grid, which is one of the samples tested in these measurements. The mesh of the sample is diamond-shaped and has all four sides equal, of length is 2.4 mm; the thickness of the aluminium wire is 0.5 mm. The sample overlaps the aperture on all sides reaching the abovementioned metallic frame where the sample is appropriately clamped in place by some screws; such an arrangement works as a sample holder. Moreover, two cement samples having a low reflectivity are also measured to show the applicability of the method SE_4 under such conditions. SE measurements from method SE_5 shown in this section use an AELA when they are referred to the aperture of size $5\,cm \times 5\,cm$ whereas they do not use an AELA when they are referred to the aperture of size $10\,cm \times 10\,cm$. When the AELA is used, it is the same aperture $5 \times 5\,cm^2$ whereas the aperture with sample is the aperture $10 \times 10\,cm^2$. Clearly, for the latter aperture, the fixture is unloaded to test the method SE_5 whereas it is loaded to test the method SE_4 according to the required conditions for the applicability of the method concerned. According to the results on SE_{ap}, the FR starts from 2 GHz for the former aperture whereas it starts from 1 GHz for the latter one.

Fig. 4 shows the coefficient of isolation I_{ns} given in (1) for the apertures of sizes $5\,cm \times 5\,cm$, $10\,cm \times 10\,cm$, and $23.3\,cm \times 13.3\,cm$. Note that $IL_{fixt,ns}$ is obtained by (6) when SE_5 is applied as only three antennas are used. For such two apertures, Fig. 4 also shows the coefficient of isolation I_s given in (3). Note that $IL_{fixt,s}$ is replaced with $IL_{fixt,pec}$, which is obtained by (8). The conditions (1) and (3) are both met; moreover, the sufficient condition (4) is also met. Fig. 5 shows $SE_{fixt,ns}$ for the apertures of size $5\,cm \times 5\,cm$ and $10\,cm \times 10\,cm$. For the latter aperture, $SE_{fixt,ns}$ is also shown with fixture loaded.

From the results in Figs. 4 and 5, one notes that the conditions are met for the applicability of the methods used below. Fig. 6 shows the SE obtained by the methods SE_5 and SE_4. For the latter method, the apertures $5 \times 5\,cm^2$ are used. For the method SE_5, an AELA is used in order to validate such a method in cases where an AELA is used as described above. Note that the cut off effect is

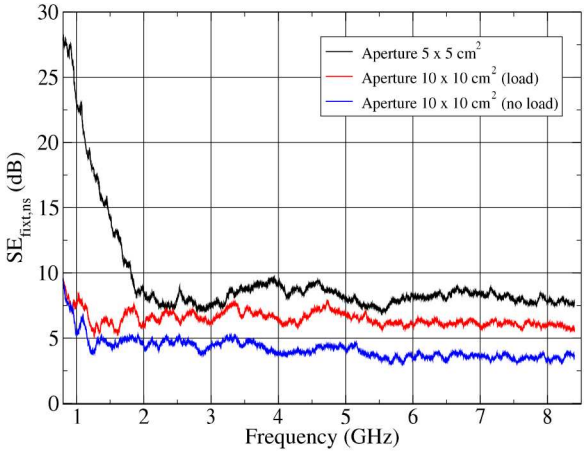

Fig. 5 *SE of the fixture with no sample for two apertures of the fixture. For the aperture* $10 \times 10\,cm^2$*, the* $SE_{fixt,ns}$ *is obtained both with load and no load in the fixture. The load is one pyramidal absorber (Eccosorb VHP-8-NRL by Emerson & Cuming)*

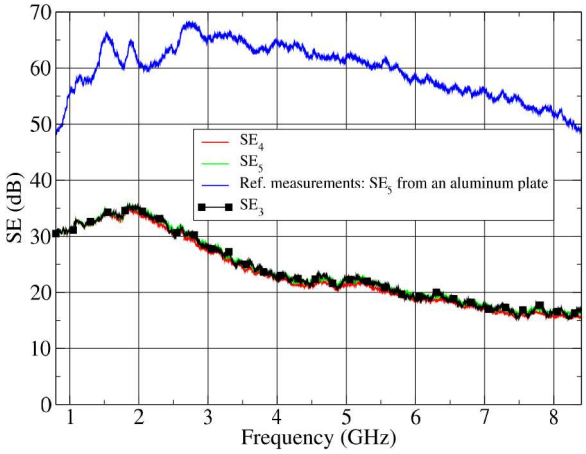

Fig. 6 *Blue and unmarked trace is the reference measurement that is the SE of an aluminium plate obtained by the method* SE_5 *when an IFBW of 100 Hz is used; it includes the leakage of the fixture. SE obtained by* SE_3*,* SE_4*, and* SE_5 *of the metallic mesh grid used as a sample. The mesh of the sample is diamond-shape and has all four sides equal, whose length is 2.4 mm. For the method* SE_5 *and* SE_4 *the aperture has size of* $5\,cm \times 5\,cm$*. For the method* SE_5 *an AELA is used in order to validate such a method in cases where an AELA is used. The AELA is the same aperture* $5 \times 5\,cm^2$ *whereas the aperture with sample is the aperture* $10 \times 10\,cm^2$*. Cutoff effect is visible for frequencies less than about 2 GHz for all three cases*

visible for frequencies less than about 2 GHz for all three methods. Fig. 7 shows the SE obtained by methods SE_5 and SE_4 for the aperture $10 \times 10\,cm^2$. Both in Figs. 6 and 7, the SE from SE_3 [4] for the same sample is also shown, as well as the reference measurement, which is the SE of a metallic plate obtained by the method SE_5; it essentially depends on the sample holder as it includes the leakage of the fixture. It is specified that the reference measurements is the same for Figs. 6–9 as shown in the corresponding captions. It is also specified that the MDR-SE given by (20) or equivalently (21), which does not include the leakage of the fixture, is not shown in such figures; it is always greater than or equal to the reference measurement from a metallic plate, as it will be also seen in Fig. 10 below.

In Figs. 6 and 7, results expected from SE_5 and SE_4 agree well with those from SE_3, which are here considered as validation results. Therefore, the method SE_5 and the condition (18) for the applicability of SE_4 are validated. In order to show the applicability of method SE_4 for sample having low reflectivity, Figs. 8 and 9 show the comparison of the SE from the SE_4 and SE_3 methods for cement samples. The aperture used for both figures is of

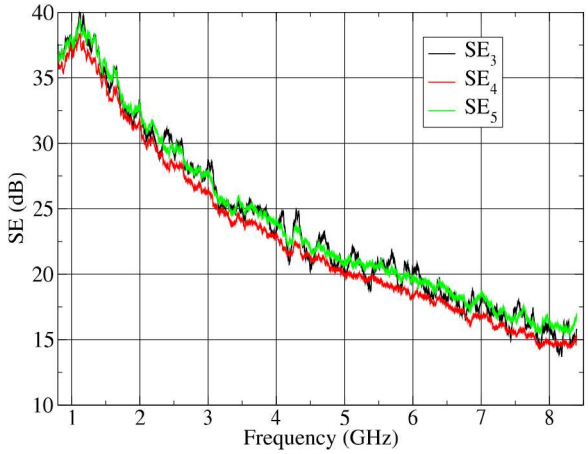

Fig. 7 *SE obtained by* SE_3*,* SE_4*, and* SE_5 *of the metallic mesh grid used as a sample. The mesh of the sample is diamond-shape and has all four sides equal, whose length is 2.4 mm. The aperture has size of* $10\,cm \times 10\,cm$*. The fixture is loaded by one pyramidal absorber (Eccosorb VHP-8-NRL by Emerson & Cuming). Cutoff effect is visible for frequencies less than about 1 GHz. The reference measurement is the same as in Fig. 6*

$23.3 \times 13.3\,cm^2$ and the sample holder is the same as that in [42, 43]. The applicability of SE_3 for such an aperture is guaranteed by the value of the isolation coefficient with no sample I_{ns} shown in Fig. 4. It should be noted that such a condition is only a necessary condition to apply SE_4. In particular, Fig. 8 shows the SE obtained by SE_3 and SE_4 for a sample formed only of commercial Portland-limestone blended cement type CEM I 52.5 R according to the European Standard EN-197/1. Fig. 9 shows the SE obtained by methods SE_3 and SE_4 for a sample formed of commercial cement, the mixture is made by the addition of graphene oxide (GO) particle. The size of the samples is the same as that of the aperture; its thickness is 3 cm.

From the results in Figs. 8 and 9, we note that SE_4 can be applied for samples having low reflectivity also when they have a non-marginal SE (see Fig. 9 in particular) as expected. In fact, samples having low reflectivity imply $IL_{fixt,s} = IL_{fixt,ns}$ and $IL_{oo,s} = IL_{oo,ns}$ in (11).

4.2 SE results from measurements made by using RC at University of Nottingham, Nottingham, England

The outer RC is a Siepel EOLE 200; it has dimensions of $4.84 \times 3.72 \times 3.11\,m^3$ and the inner chamber has dimensions of $0.36 \times 0.45 \times 0.54\,m^3$. The sample holder aperture is $0.05\,m \times 0.05\,m$ and is situated in a thick brass plate. The sample overlaps the aperture on all sides and it is clamped in place by a brass frame with 16 screws. Inside the outer chamber, the input electromagnetic field is randomised by means of hybrid stirring using one big metallic stirrer, which works in step mode for measurements used in this paper, and FS; inside the inner chamber, only FS is used. The measurement setup includes a two-port VNA, model Agilent PNA E8362B and three antennas. The two receiving antennas, whose one is inside the outer chamber ($R_{x,o}$) and the other one inside the inner chamber ($R_{x,i}$), are two equal double-ridge horn antennas, model AH systems SAS-571. The third antenna is an ETS Lindgren double-ridged horn antenna, model 3115, which is used as a transmitting antenna (T_x) in the outer chamber. The NRCs is shown in Fig. 11.

The VNA used for measurements has two ports. The transmitting antenna was permanently connected to the port 1 by appropriate cables and connectors, whereas the two receiving antennas were alternatively connected to the port 2 by appropriate cables and connectors. It is specified that the two receiving antennas are connected to the port 2 by the same overall cable, excepting for a short cable (75 cm long) that connects the antenna inside the fixture to the bulkhead connector, which passes through a wall of the fixture. Considering that SE_5 is not rigorously self-

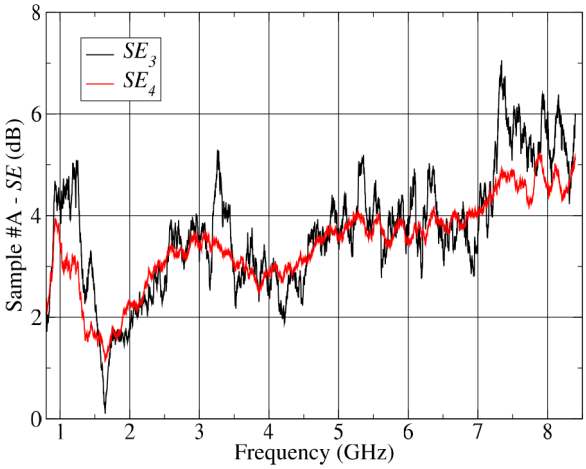

Fig. 8 *SE evaluated by SE_3 and SE_4 methods for a commercial sample of Portland-limestone blended cement type CEM I 52.5 R. The aperture has size of 23.3 cm × 13.3 cm. The reference measurement is the same as in Fig. 6*

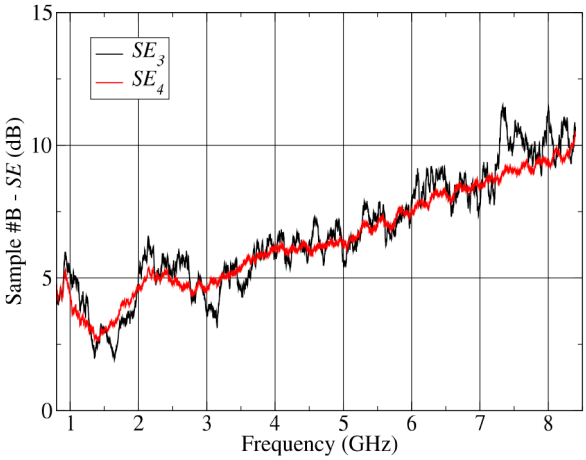

Fig. 9 *SE evaluated by SE_3 and SE_4 methods for a commercial sample of Portland-limestone blended cement type CEM I 52.5 R with GO. The aperture has size of 23.3 cm × 13.3 cm. The reference measurement is the same as in Fig. 6*

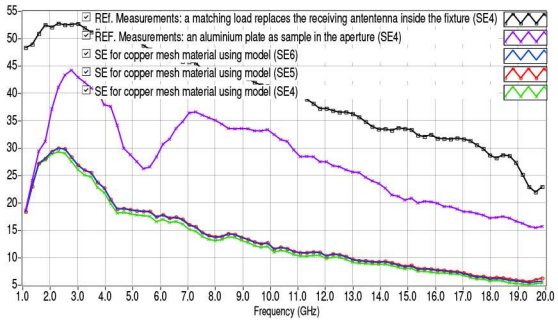

Fig. 10 *SE of the copper mesh. Black and square-marked trace is the MDR obtained by a matched load when an IFBW of 3 kHz is used; violet and cross-marked trace is the reference measurement, which includes the leakage of the fixture. Blue and unmarked, red and circle-marked, and green and cross-marked traces are the SE of the copper mesh, achieved by SE_5, SE_6, and SE_4 methods. Cutoff effect is visible for frequencies less than about 2 GHz*

calibrating, the measurement system is calibrated by two separate 'Thru' calibrations, which are made between the references plane of T_x and $R_{x,o}$ and between the references plane of T_x and $R_{x,i}$, respectively.

Measurements are made for 120 positions of the stirrer, which are evenly spaced in angle. For each stirrer position 16,001 point in

Fig. 11 *Inside of the RC at University of Nottingham. The fixture is well visible in the chamber*

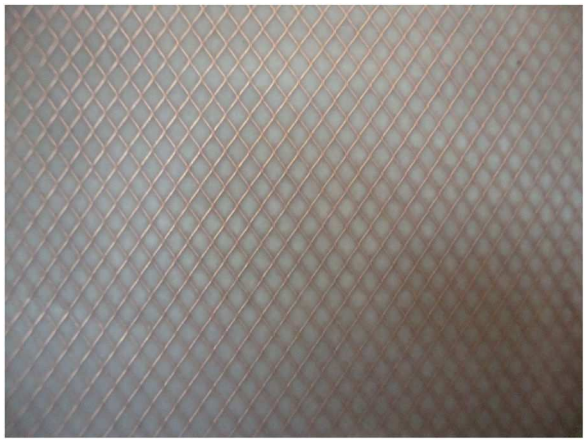

Fig. 12 *Geometrical details on the tested copper mesh*

frequency is acquired by the VNA. The FR was set from 1 to 20 GHz; the IFBW is set to 3 kHz; the port power is set to 0 dBm. The SF is 1.1875 MHz. The transmission coefficients inside the outer chamber and that between outer and inner chambers are measured both with no sample and with the sample in the aperture. Measurements on a metallic plate and for MDR were also made.

The sample tested is referred to as 'copper mesh'. It is described as follows: expanded copper foil (110 copper); diamond-shaped unit cell; copper thickness: 0.076 mm; copper strand width: 0.178 mm; diamond long dimension 3.2 mm; diamond short dimension 2.1 mm. Fig. 12 shows geometrical details on the copper mesh.

Even though results are shown across the whole FR of acquisition (from 1 to 20 GHz), it is important to note that the cutoff is visibly present for frequencies less than about 2 GHz, whereas the specifics of the antennas are not known for frequencies >18 GHz. The latter issue is not very important when the impedance matching holds and tests are made in an RC as in our case. It is specified that the FSB used for data processing is 200 frequency points; it corresponds to (199 × 1.1875) = 236.3 MHz.

Fig. 13 shows that the condition (18) or equivalently (19) is met. The condition (19) implies an error of 0.75 dB on SE_4, if we consider a value of 8 dB for $SE_{fixt,ns}$. Hence the conditions for the applicability of SE_5 and SE_6 are also met. In Fig. 10 are shown five traces. The black-coloured trace represents MDR-SE given by (20) or equivalently (21), which are equivalent to (22) in this case; it does not include the leakage of the fixture. The violet-coloured trace represents the reference measurement of the measurement

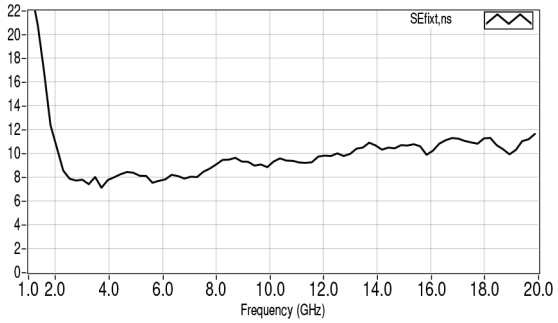

Fig. 13 *SE of the fixture $SE_{fixt,ns}$. Cutoff effect is visible for frequencies less than about 2 GHz*

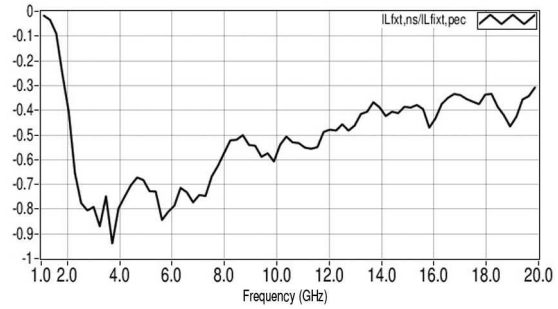

Fig. 14 *Ratio $IL_{fixt,ns}/IL_{fixt,pec} = SE_4/SE_6$. Cutoff effect is visible for frequencies less than about 2 GHz*

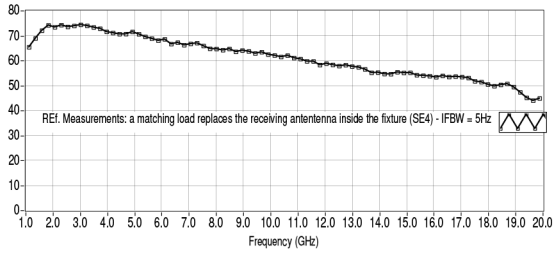

Fig. 15 *MDR obtained by a matched load when an IFBW of 5 Hz is used*

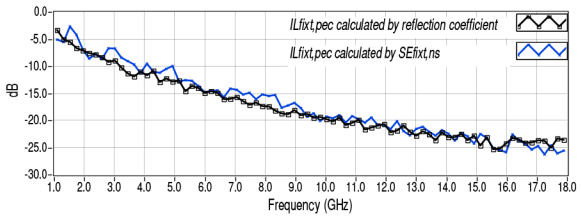

Fig. 16 *$IL_{fixt,pec}$ comparison. $IL_{fixt,pec}$ achieved by (6)–(8) and that by measurements of the reflection coefficient. IFBW is 3 kHz in these measurements*

setup. It essentially depends on the sample holder that reduces the edge leakage of the sample. The latter also determines the behaviour of the trace between 4 and 7 GHz. The blue-coloured, red-coloured, and green-coloured traces represent the SE of the copper mesh achieved by using the three different methods SE_5, SE_6, and SE_4, which are given by (10), (13), and (15), respectively, as mentioned above.

Fig. 14 shows the ratio $IL_{fixt,ns}/IL_{fixt,pec}$, which is the same as the ratio SE_4/SE_6. Finally, Fig. 15 shows the reference measurements using the matching load where the IFBW is 5 Hz. It can be noted the increase of such a reference with respect to that shown in Fig. 15 where IFBW is 3 kHz.

We note that results from SE_5 and SE_6 are practically overlapped whereas results from SE_4 are slightly below the first two. The slight difference between SE_5, SE_6 and SE_4, which is generally <1 dB, is consistent with that expected (–0.75 dB). We note also that when $SE_{fixt,ns}$>10 dB, as it is for frequencies <2 GHz, the error on SE_4 reduces and the traces concerning SE_5, SE_6, and SE_4 are practically all overlapped even though a considerable cutoff effect is present for such frequencies.

From results, the cutoff effect of the aperture with sample holder is well visible for frequencies less than about 2 GHz as expected. Results from traces SE_5, SE_6, and SE_4 implicitly show the validity of the corresponding methods.

4.3 SE of a gasket from measurements made by using the RC at University 'Parthenope', Napoli, Italy

In this section, results of SE of a gasket is shown. The gasket is a non-woven fabric. Also, MDR is determined; it is obtained by (20) or equivalently (21). The SE of the gasket is obtained both by SE_5 (9) and [10, (1)]. Results from the two methods are also compared. For the application of SE_5, $IL_{fixt,pec}$ is achieved by using the same measurements acquired for $SE_{fixt,ns}$ in [10], where de facto an AELA of 10 cm by 10 cm is used, whereas $SE_{fixt,s}$ is achieved by using the measurements acquired for results in [44]. For the application of [10, (1)], the same measurements for $SE_{fixt,s}$ in [44] are used whereas $IL_{fixt,s}$ is achieved by using measurements in [10].

Note that all requested conditions to apply the method SE_5 and [10, (1)] are met. It is specified that the IFBW is 2 Hz for the measurements of $IL_{0,i,s}$ and $IL_{o,i,T}$ in order to adequately increase the MDR as a high MDR is necessary for such measurements. Measurements made by an IFBW of 2 Hz and 16,000 samples take 2 h about for a FR from 1 to 18 GHz. It is also specified that the two receiving antennas, which are positioned inside the fixture and the RC, are equal. To be more precise, they are two double-ridge waveguide horn antennas for measurements of $SE_{fixt,ns}$ [10] and two monopole antenna for measurements of $SE_{fixt,s}$ [44]. It is also recalled that the fixture has a removable side, so that the aperture is one full side of the fixture; the window is equipped with a flange that in turn is covered by the gasket; finally, the removable wall is positioned on the gasket. The gasket is fixed to the flange, whose width is 0.04 m, by adhesive aluminium, which is applied both on the internal walls and on the underside of the flange itself, in order to optimise the performance of the gasket. The leakage of the fixture is minimised as it is configured for the SE measurement of gaskets. No mechanical stirrer is present inside the fixture; only FS is used inside the fixture. The single antenna inside the fixture is fed through a coaxial cable and an N-female–female bulkhead connector. The bulkhead connector, which has a circular flange, is appropriately fixed in a wall by a nut and the gasket; the latter is the same as that positioned on the flange and it is accurately put on both internal and external sides. Therefore, the aluminium cover slab is appropriately positioned to close the fixture by a robust frame and some clamps [10, 44]. The frame uniformly distributes the pressure made by twelve tightened clamps. For the application of [10, (1)], reflection measurements, which require a single antenna in the fixture, were used to obtain $IL_{fixt,pec}$ [10]. The use of a single antenna inside the fixture has generally the critical issues in the measurements of the reflection coefficients, as mentioned above, and in the use of the '2' to calculate $IL_{fixt,pec}$ [10]. However, these specific measurements of $IL_{fixt,pec}$ were acquired outside the RC in order that the minimum length of the cables was used, even though it is not expressly specified in [10]. Fig. 16 shows $IL_{fixt,pec}$ achieved by the application of (6)–(8) and the corresponding result obtained by measurements of the reflection coefficient and application of [10, (10)].

Fig. 17 shows SE_g, which denotes the SE of the gasket, achieved by the application of SE_5 (9) and the corresponding result obtained by application of [10, (1)]. In the same figure the SE obtained by replacing the receiving antenna in the fixture with a matched load is also shown. It represents the MDR of the measurement system without including the leakage of the fixture as specified above. It is specified that the measurements using the termination are made without the cover. These results suggest repeating the measurements by using the termination with the fixture closed by the metallic cover; that is, the same measurement configuration for the gasket should be used except that the antenna

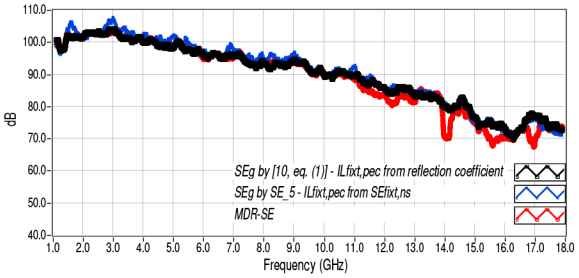

Fig. 17 *Comparison between SE_g and MDR. Procedures for [10, (1)] (red trace) and for SE_5 (blue trace) are used. Black and square-marked trace represents SE_g from [10, (1)] where $IL_{fixt,pec}$ is achieved by measurements of the reflection coefficient; blue and cross-marked trace represents SE_g from SE_5 where $IL_{fixt,pec}$ is achieved by (6)–(8). Red and circle-marked trace represents MDR-SE. IFBW is 2 Hz in these measurements*

inside the fixture is replaced with a matching load. It is important to note that the term $IL_{o,i,s}$ increases and $SE_{fixt,s}$ decrease for SE measurements of gaskets at the same fixture volume with the increase of the aperture size. This decrease tends to be compensated by the increase of the aperture size as (9), or equivalently (10), shows, so that SE_g is forced to be constant regardless of the aperture size. Nevertheless, the SE of gaskets may depend on the aperture size as the geometrical area to be considered it is not normally determinable [10]. Therefore, for SE of gaskets only, it is suggested that the aperture size and the perimeter concerned be shown in the technical report of measurements. The problem certainly exists and it is greater when the method in [1, eq. G.5] is used as no compensation is present in it. On the other hand, to the best of our knowledge, no theory has been published in support of such a method [10, 45]. We note that results from method SE_5 and general method [10, (1)] match very well again. According to [1, Section G.5.1], the SE can also be measured in terms of average TCS with sample only, where the TCS is denoted by σ_a instead of $\sigma_{t,s}$ [4]. It is important to note that the SE values expressed by [1, eq. G.7] are not normalised; so, they depend inevitably on the size of the aperture. One also notes that [10, (1)] divided by $A_a/4\ \mathrm{m}^2$ is equal to the inverse of [1, eq. (G.7)]. In the latter case, the corrections for the efficiencies of the antennas are clarified. Therefore, [1, eq. G.7] gives SE values quantitatively greater than those given by [10, (1)], SE_5, (9) and (10), and SE_4 (15); the difference is $-10\log(A_a/4)$, which is $-10\log(0.5^2/4) = 12.04\ \mathrm{dB}$ in our case. However, the difference depends inevitably on the geometrical area of the aperture as [1, eq. G.7] has no normalisation. It is reaffirmed that in order to avoid any leakage unconnected to the gasket, only the FS is used to stir the field inside the fixture. The results show that the non-woven fabric can be advantageously used as gasket, including being applied to achieve fixtures for SE measurements in an RC, as it is very effective and easy to apply.

5 Discussion and conclusions

In this paper, some developments on the SE measurements of gaskets and materials in RCs are shown in order to contribute to the improvement the annex G in the Standard IEC 64000-4-21. A variant method, which is denoted by SE_5, where only three antennas are requested, is shown. It is shown in two versions: one requires an AELA and the other not. This procedure is appropriate for gaskets and for any flat material having a sufficiently high reflectivity at least on one side. The applicability of the simplest method SE_4 is enhanced by a simple and usable condition, as well as by particular cases where it can be directly applied for samples having low reflectivity and absorption as shown by results in Figs. 8 and 9. This method can be used for gaskets and any flat sample and requires only two antennas. Comparisons of results support the methods for the SE measurements of gaskets and material in RCs shown in this paper. It is specified that the verification of the condition under which the simplest method SE_4 is applicable, which is made only once for a given measurement setup including the chambers, requires three antennas. However, for two equal CRCs, such a condition can be verified by using only two antennas. Moreover, for such a chamber system, by using the methods SE_5 and SE_4, a powerful facility can be obtained for SE measurement using only two antennas. This has not been developed here both for lack of such a chamber system at this time and for brevity. Finally, we note that by using chambers with volumes and apertures appropriately reduced, the measurement FR could be extended to some tens of GHz including frequencies for 5G communication system, where the simplest model is the most appropriate to be used. By considering these last two points, the applications of the SMART^{TM} 800 Dual Reverberation Test Cell from ETS-LINDGREN [46] could be increased and improved.

6 Acknowledgment

This work was supported by the STSM Grant from COST Action IC1407. Angelo Gifuni wishes to thank the Director of Engineering Department Prof. Vito Pascazio for his valuable support to this work.

7 References

[1] 'Electromagnetic compatibility (EMC) – part 4-21: Testing and measurement techniques – reverberation chamber test methods', Geneva, Switzerland, 2011

[2] Hatfield, M.O.: 'Shielding effectiveness measurements using mode stirred chambers: a comparison of two approaches', *IEEE Trans. Electromagn. Compat.*, 1988, **30**, pp. 229–238

[3] Loughry, T.A., Gurbaxani, S.H.: 'The effects of intrinsic test fixture isolation on material shielding effectiveness measurements using nested mode-stirred chambers', *IEEE Trans. Electromagn. Compat.*, 1995, **37**, (3), pp. 449–452

[4] Holloway, C.L., Hill, D.A., Ladbury, J., *et al.*: 'Shielding effectiveness measurements of materials using nested reverberation chambers', *IEEE Trans. Electromagn. Compat.*, 2003, **45**, (2), pp. 350–356

[5] Leo, R.D., Gradoni, G., Mazzoli, A., *et al.*: 'Shielding effectiveness evaluation of densified-small-particles (DSP) cement composite'. 2008 Int. Symp. on Electromagnetic Compatibility – EMC Europe, Hamburg, Germany, 2008, pp. 1–6

[6] Mariani Primiani, V., Moglie, F., Pastore, A.P.: 'Field penetration through a wire mesh screen excited by a reverberation chamber field: FDTD analysis and experiments', *IEEE Trans. Electromagn. Compat.*, 2009, **51**, (4), pp. 883–891

[7] Lampasi, D., Sarto, M.: 'Shielding effectiveness of a thick multilayered panel in a reverberating environment', *IEEE Trans. Electromagn. Compat.*, 2011, **53**, (3), pp. 579–588

[8] Leferink, F., Serra, R., Schipper, H.: 'Microwave-range shielding effectiveness measurements using a dual vibrating intrinsic reverberation chamber'. 2012 42nd European Microwave Conf., Amsterdam, Netherlands, 2012, pp. 344–347

[9] Gifuni, A., Migliaccio, M.: 'Use of nested reverberating chambers to measure shielding effectiveness of nonreciprocal samples taking into account multiple interactions', *IEEE Trans. Electromagn. Compat.*, 2008, **50**, (4), pp. 783–786

[10] Gifuni, A.: 'A proposal to improve the standard on the shielding effectiveness measurements of materials and gaskets in a reverberation chamber', *IEEE Trans. Electromagn. Compat.*, 2017, **59**, (2), pp. 394–403

[11] Ladbury, J., Hill, D.A.: 'Enhanced backscatter in a reverberation chamber: inside every complex problem is a simple solution struggling to get out'. 2007 IEEE Int. Symp. on Electromagnetic Compatibility, Hawaii, USA, 2007, pp. 1–5

[12] Holloway, C.L., Shah, H.A., Pirkl, R.J., *et al.*: 'Reverberation chamber techniques for determining the radiation and total efficiency of antennas', *IEEE Trans. Electromagn. Compat.*, 2012, **60**, (4), pp. 1758–1770

[13] Tian, Z., Huang, Y., Xu, Q.: 'Efficient methods of measuring shielding effectiveness of electrically large enclosures using nested reverberation chambers with only two antennas', *IEEE Trans. Electromagn. Compat.*, 2017, **59**, (6), pp. 1872–1879

[14] Hill, D.A., Ma, M.T., Ondrejka, A.R., *et al.*: 'Aperture excitation of electrically large, lossy cavities', *IEEE Trans. Electromagn. Compat.*, 1994, **36**, (3), pp. 169–178

[15] Gifuni, A.: 'On the measurement of the absorption cross section and material reflectivity in a reverberation chamber', *IEEE Trans. Electromagn. Compat.*, 2009, **51**, (4), pp. 1047–1050

[16] Gradoni, G., Micheli, D., Moglie, F., *et al.*: 'Absorbing cross section in reverberation chamber: experimental and numerical results', *Progress Electromagn. Res. B.*, 2012, **45**, pp. 187–202

[17] Gifuni, A.: 'Relation between the shielding effectiveness of an electrically large enclosure and the wall material under uniform and isotropic field conditions', *IEEE Trans. Electromagn. Compat.*, 2013, **55**, (6), pp. 1354–1357

[18] Hallbjorner, P., Carlberg, U., Madsen, K., *et al.*: 'Extracting electrical material parameters of electrically large dielectric objects from reverberation chamber measurements of absorption cross section', *IEEE Trans. Electromagn. Compat.*, 2005, **47**, (2), pp. 291–303

[19] Gifuni, A.: 'On the expression of the average power received by an antenna in a reverberation chamber', *IEEE Trans. Electromagn. Compat.*, 2008, **50**, (4), pp. 1021–1022
[20] Flintoft, I.D., Melia, G.C.R., Robinson, M.P., *et al.*: 'Rapid and accurate broadband absorption cross-section measurement of human bodies in a reverberation chamber', *Meas. Sci. Technol.*, 2015, **26**, (6), p. 065701
[21] Gifuni, A., Khenouchi, H., Schirinzi, G.: 'Performance of the reflectivity measurement in a reverberation chamber', *Prog. Electromagn. Res.*, 2015, **154**, pp. 87–100
[22] Corredores, Y., Besnier, P., Castel, X., *et al.*: 'Adjustment of shielding effectiveness, optical transmission, and sheet resistance of conducting films deposited on glass substrates', *IEEE Trans. Electromagn. Compat.*, 2017, **59**, (4), pp. 1070–1078
[23] Koch, G., Kolbig, K.: 'The transmission coefficient of elliptical and rectangular apertures for electromagnetic waves', *IEEE Trans. Antennas Propag.*, 1968, **16**, (1), pp. 78–83
[24] Butler, C., Rahmat Samii, Y., Mittra, R.: 'Electromagnetic penetration through apertures in conducting surfaces', *IEEE Trans. Antennas Propag.*, 1978, **26**, (1), pp. 82–93
[25] Gifuni, A., Ferrara, G., Migliaccio, M., *et al.*: 'Estimate of the shielding effectiveness of an electrically large enclosure made with pierced metallic plate in a well-stirred reverberation chamber', *Progr Electromagn Res C*, 2013, **44**, pp. 133–144
[26] Migliaccio, M., Ferrara, G., Gifuni, A., *et al.*: 'Shielding effectiveness tests of low-cost civil engineering materials in a reverberating chamber', *Progress Electromagn. Res. B*, 2013, **54**, p. 227
[27] Altun, M., Karteri, I., Güne, M.: 'A study on EMI shielding effectiveness of graphene based structures'. 2017 Int. Artificial Intelligence and Data Processing Symp. (IDAP), Malatya, Turkey, 2017, pp. 1–5
[28] Chiu, C., Chang, Y., Hsieh, H., *et al.*: 'Suppression of spurious emissions from a spiral inductor through the use of a frequency-selective surface', *IEEE Trans. Electromagn. Compat.*, 2010, **52**, (1), pp. 56–63
[29] Syed, I.S., Ranga, Y., Matekovits, L., *et al.*: 'A single-layer frequency-selective surface for ultrawideband electromagnetic shielding', *IEEE Trans. Electromagn. Compat.*, 2014, **56**, (6), pp. 1404–1411
[30] Taylor, B.N., Kuyatt, C.E.: '*Guidelines for evaluating and expressing the uncertainty of NIST measurement results*' (Physics Laboratory National Institute of Standards and Technology, USA, 1994), NIST Tech Note 1297
[31] Arnaut, L.R.: 'Measurement uncertainty in reverberation chambers', Sample statistics NPL Report TQE2 2nd edition, 2008, pp. 1–136
[32] Gifuni, A., Ferrara, G., Sorrentino, A., *et al.*: 'Analysis of the measurement uncertainty of the absorption cross section in a reverberation chamber', *IEEE Trans. Electromagn. Compat.*, 2015, **57**, (5), pp. 1262–1265
[33] Blumenfeld, D.: '*Operations research calculations handbook*' (CRC Press, USA, 2001)
[34] Gifuni, A., Flintoft, I.D., Bale, S.J., *et al.*: 'A theory of alternative methods for measurements of absorption cross section and antenna radiation efficiency using nested and contiguous reverberation chambers', *IEEE Trans. Electromagn. Compat.*, 2016, **58**, (3), pp. 678–685
[35] Gifuni, A., Bastianelli, L., Moglie, F., *et al.*: 'Base-case model for measurement uncertainty in a reverberation chamber including frequency stirring', *IEEE Trans. Electromagn. Compat.*, 2018, **60**, (6), pp. 1695–1703
[36] Gifuni, A., Bastianelli, L., Migliaccio, M., *et al.*: 'On the estimated measurement uncertainty of the insertion loss in a reverberation chamber including frequency stirring', *IEEE Trans. Electromagn. Compat.*, 2019, **61**, (5), pp. 1414–1422
[37] Aan Den Toorn, J., Remley, K.A., Holloway, C.L., *et al.*: 'Proximity-effect test for lossy wireless-device measurements in reverberation chambers', *IET Sci., Meas. Technol.*, 2015, **9**, (5), pp. 540–546
[38] Höijer, M., Kroon, L.: 'Field statistics in nested reverberation chambers', *IEEE Trans. Electromagn. Compat.*, 2013, **55**, (6), pp. 1328–1330
[39] Salo, J., El-Sallabi, H.M., Vainikainen, P.: 'The distribution of the product of independent Rayleigh random variables', *IEEE Trans. Antennas Propag.*, 2006, **54**, (2), pp. 639–643
[40] Kovalevsky, L., Langley, R.S., Besnier, P., *et al.*: 'Experimental validation of the statistical energy analysis for coupled reverberant rooms'. 2015 IEEE Int. Symp. on Electromagnetic Compatibility (EMC), Dresden, Germany, 2015, pp. 546–551
[41] Gradoni, G., Antonsen, T.M., Anlage, S.M., *et al.*: 'Random coupling model for interconnected wireless environments'. 2014 IEEE Int. Symp. on Electromagnetic Compatibility (EMC), North Carolina, USA, 2014, pp. 792–797
[42] Bastianelli, L., Mariani Primiani, V., Moglie, F., *et al.*: 'Experimental analysis of the aging effects on shielding effectiveness of cementitious composites'. 2018 IEEE Symp. on Electromagnetic Compatibility, Signal Integrity and Power Integrity (EMC, SI PI), California, USA, 2018, pp. 71–75
[43] Bastianelli, L., Capra, S., Gradoni, G., *et al.*: 'Shielding effectiveness statistical evaluation of random concrete composites'. Int. Workshop on Metrology for AeroSpace, Florence, Italy, 2016
[44] Gifuni, A., Grassini, G.: 'Shielding effectiveness measurements of a metallic fixture where a non-woven fabric is used as gasket in a reverberation chamber'. Fondazione Giorgio Ronchi, n. 5, 2016
[45] Fan, W., Panitz, M., Greedy, S., *et al.*: 'On the shielding effectiveness measurements of building materials at radio communication frequencies in reverberation chambers'. 2010 Asia-Pacific Int. Symp. on Electromagnetic Compatibility, Beijing, China, 2010, pp. 1622–1625
[46] 'http://www.ets-lindgren.com/products/chambers/emc-chambers/smart%e2%84%a2-reverb-chambers/14000/1400006'